Korean J. Chem. Eng.
DOI: 10.1007/s11814-015-0018-x

pISSN: 0256-1115
eISSN: 1975-7220

A comprehensive study (kinetic, thermodynamic and equilibrium) of arsenic (V) adsorption using $KMnO_4$ modified clinoptilolite

Mohamadreza Massoudinejad*, Anvar Asadi,†, Mehdi Vosoughi***, Morteza Gholami****, Babak kakavandi***, and Mohammad Amin Karami*****

*Department of Environmental Health and Member of Safety Promotion and Injury Prevention Research Center, Shahid Beheshti University of Medical Science, Tehran, Iran
**Department of Environmental Health Engineering, School of Public Health, Student's Research Committee, Shahid Beheshti University of Medical Sciences, Tehran, Iran
***Department of Environmental Health Engineering, School of Health, Ahvaz, Jundishapur University of Medical Sciences, Ahvaz, Iran
****Department of Chemistry, University of Golestan, Gorgan, Iran
*****Department of Environmental Health Engineering, School of Health, Ilam University of Medical Science-Environment Research Center, Isfahan University of Medical Sciences (IUMS), Isfahan, Iran
(*Received 12 August 2014 • accepted 23 January 2015*)

Abstract−The sorption of As(V) on manganese oxide coated zeolite (MOCZ) was investigated through batch study to explore the feasibility of removing arsenic from groundwater. MOCZ was characterized by scanning electron microscopy, XRD, FTIR spectroscopy, and point of zero charge (pH_{PZC}) measurements. The effects of process parameters such as contact time, adsorbent size, temperature and pH were investigated. Arsenic detection was carried out by atomic fluorescence spectrometer. Arsenate adsorption onto MOCZ followed the pseudo-second-order kinetic model with a correlation coefficient more than 0.99. Optimum removal of arsenate occurred within pH range of 6-10. The equilibrium data were analyzed by Langmuir, Freundlich and Dubinin-Radushkevich (D-R) isotherm models. The maximum adsorption capacity calculated from the Langmuir and D-R models was 151 and 152.8 μg g^{-1}, respectively, at 38 °C. The activation energy of adsorption (E_a) was found to be 3.68 kj mol^{-1}, suggesting that the adsorption process may be physical sorption. Thermodynamic parameters: ΔH^o, was 1.181 kj mol^{-1}; ΔS^o, was −0.29 kj mol^{-1}, while the values of ΔG^o were −83.9, −86.7 and 89.8 kj mol^{-1} at 18, 28 and 38, respectively, suggesting endothermic and spontaneous process and a rise in temperature favoring the adsorption.

Keywords: Manganese Oxide, Arsenic (V), Adsorption, Equilibrium, Thermodynamics, Kinetics, Desorption

INTRODUCTION

Arsenic is semi-metallic element which occurs naturally in environment in many parts of the world [1,2]. There are four main oxidation states of arsenic, −3, 0, +3 and +5, of which trivalent arsenit (As^{3+}) and pentavalent arsenate (As^{5+}) are mainly dominant in natural water [3]. The predominant valence of arsenic depends on redox potential of geological environment [3,4]. Countries around the world are exposed to arsenic and a primary concern for exposure is via drinking water. Arsenic causes diseases like hyper pigmentation, skin and liver cancer, blackfoot, nervous disorder and respiratory disorder [5-7]. Arsenic concentration in drinking water in some countries like Bangladesh (up to 2,500 g/L), Argentina (up to 7,750 mg/L), United States (up to 3,100 mg/L) and Iran (up to 1,024 mg/L) is very high and the United State Environmental Protection Agency (USEPA) and World Health Organization (WHO) set standard and guideline level of 10 mg/L for it, respectively [8]. Because of difficulties in removing arsenic to that level, some countries such as Bangladesh and Iran still have 50 mg/L as standard level [7,8]. In order to remove arsenic concentration in drinking water, water treatment for its remediation has become a very important environmental issue [4,6].

A number of techniques such as ion exchange [11], membrane filtration [12], adsorption [13], and flocculation, coagulation and precipitation [14] have been used for removal of arsenic from water. Among others, adsorption is generally considered to be promising and effective method for removal of arsenic from water due to easy operation and management, less sludge production and its regeneration capability [4,5,15]. Naturally occurring zeolites and their modification form such as hydrated aluminosilicate materials, bentonite and kaoline have been used extensively due to their low cost and availability in large amounts on the earth [4,15,16].

Both natural and synthetic clinoptilolite modified have been studied for sorption of pollutants in recent years [17-20]. To improve the zeolite performance, e.g., adsorption capacity and increased mechanical and resistance to chemical environment, several modification

†To whom correspondence should be addressed.
E-mail: anvarasadi@sbmu.ac.ir, asadia66@gmail.com

methods including iron modification [4], surfactant modification [21], and lanthanum modification have been used [6,22]. One of these surface coating methods is use of manganese oxides, which provides large surface area, microporous structure and high ability to adsorb ions such as As(V) [23,24]. Anyways, manganese oxide is available only as fine powder or produced in aqueous suspension in the form of hydroxide or gels [23]. The use of manganese oxides as adsorbents in form of powder has practical limitations, such as hardness solid/liquid separation, high pressure drop and leaching of metal/metal oxide in final treated water. Thus, to overcome these problems, manganese oxide can be coated on clinoptilolite surface to provide an effective adsorbent for arsenic removal from water [23,25,26]. It appears that this method provides an effective surface and may increase the arsenic removal from water.

This work is continuation of a wide project on the activation of a natural Iranian zeolite to be used as adsorbent of heavy metal ions. Present study evaluates the properties of manganese oxide coated zeolite as an adsorbent for removing As(V) ions from synthetic solution in batch laboratory system. The effects of various operating conditions such as pH, zeolite mesh size, contact time and initial arsenic concentration were investigated. The kinetics and sorption isotherms were also studied. The physiochemical characteristics of MOCA were explored with SEM, X-ray diffraction (XRD), FTIR and point of zero charge (pH_{pzc}) measurements.

EXPERIMENTAL

1. Materials and Reagents

The zeolite used was a clinoptilolite-rich tuff obtained from the Semnan province, Iran with a grain size range 1-5 mm. The zeolite sample was crushed and sieved to the average particle diameter of 1, 2 and 5 mm (18, 10 and 4 US mesh). The chemical formula of zeolite based on XRD was $(Na_{0.52}K_{2.44}Ca_{1.48})$ $(Al_{6.59}Si_{29.41}O_{72})$. $28(H_2O)$ with Si/Al=4.46, that almost meets the ideal ratio. A stock solution of 100 mg L^{-1} of As(V) was prepared by dissolving 0.417 g of $Na_2HAsO_4{\cdot}7H_2O$ (Sigma-aldrich, USA) in de-ionized water and was used to prepare the sorbate solution at concentration 0.1, 0.2, 0.5, 1, 2, and 3 mg L^{-1} by appropriate dilution. Potassium permanganate (Sigma-Aldrich, USA) and HCl (Merck) were used to prepare the MOCZ.

2. Potassium Permanganate Modification

The external surface of clinoptilolite was modified by potassium permanganate through a similar procedure proposed by Taffarel and Rubio [25]. The modification procedure was as follows:

1. Zeolite was washed with deionized water and drying at room temperature.

2. Zeolite was converted to its Na form by suspending 50 g into 500 ml of a 2 M NaCl solution for a period of 24 h.

3. The zeolite suspension was separated and washed several times to remove chloride ions (moher test) and then dried at room temperature.

4. The dried Na-zeolite sample was placed in a backer containing KMnO4, then HCl (37.5%) was add dropwise into the solution. After stirring for 1 h at 90 °C, the zeolite was separated, washed several times with distilled water (in order to remove Cl^- and K^+) until the runoff was clear, then dried in oven at 100 °C for 24 h and stored in a polypropylene bottle for further use.

3. Characterization of Adsorbent

SEM photomicrography of the external surface of uncoated zeolite and manganese oxide coated zeolite was taken using a KYKY (EM-3200) microscope. X-ray diffraction (XRD) analysis was performed on the zeolite (modified) to confirm the crystal structure and determination of the mineralogical composition. Powder diffractograms of the zeolite were obtained with a PANalytical X'Pert Pro MPD diffractogram equipped with Cu Kα radiation. FTIR spectroscopy of the zeolitic phase, before and after adsorption process was obtained. FTIR analysis was conducted in a WQF-510A/520A FTIR Spectrometer; the samples were prepared using the KBr pressed-disk technique, with 1% inclusions of the sample to be analyzed.

The point of zero charge (pH_{PZC}) of the samples was carried out as follows [25,26]: 50 ml of 0.01 M NaCl solution was placed in a closed Erlenmeyer flask. To stabilize the pH and prevent CO_2 dissolution nitrogen was bubbled through the solution. The pH was adjusted to a value between 2 and 12 by adding HCl 0.1 M or NaOH 0.1 M solutions. The zeolite sample (0.15 g) was added and the final pH was measured after 24 h under agitation at room temperature. The pH_{pzc} is the point where the curve pH_{final} vs. pH_{inital} crosses the line $pH_{initial}=pH_{final}$.

4. Effect of pH on Arsenic Adsorption

The influence of pH on arsenic adsorption by MOCZ was evaluated at acidic, neutral and basic condition. The pH of seven 100 ml solutions of 1 mg/L arsenic was adjusted to the value ranging from 2-12 by adding 0.1 M HCl or 0.1 M NaOH. One gram of MOCZ was added to the solution in high-density polyethylene plastic bottle and placed in a shaker and allowed to equilibrate for 3 h at 200 rpm. The samples were removed from the shaker, final pH-values were recorded and arsenic analysis was performed with AF-640 Atomic fluorescence spectrometer (BRAIC) for As(V) concentration.

5. Methods of Adsorption Studies

For As(V) sorption, 1.0 g of MOCZ was mixed with 100 ml of As(V) solutions with initial concentration range from 0.1 to 3 mg/L in high-density polyethylene plastic bottles. The mixture was placed in a shaker at 200 rpm for 3 h. The supernatant was analyzed for equilibrium As(V) solution concentration. For kinetic study, 1.0 g of MOCZ was mixed with 100 ml of 1 mg/L solution and then stirred for different periods of time (5, 15, 30, 60, 120, 180 and 300 min) at initial pH of 6.5-7. The supernatant was centrifuged and filtered through a 0.2 μm filter before As(V) concentration analysis. The adsorption studies of As(V) onto MOCZ were carried out with the same procedure during 180 min (enough time for reaching chemical equilibrium) and varying initial concentration (0.1-3 mg/L). The uptake (q) of arsenic expressed as As(V) removal per unit mass of MOCZ (μg As/g) at time t was calculated using Eq. (1)

$$q_t = \frac{(C_0 - C_t)V}{m} \quad (1)$$

where C_0 and C_t are the As(V) initial and equilibrium concentration (μg L^{-1}) at time t, V is the solution volume (L), and m is the adsorbent dose (g).

6. Kinetic and Thermodynamic and Isotherm Studies

6-1. Kinetic Parameters

To evaluate the efficiency of arsenic mass transfer to MOCZ and

potential rate controlling step, the kinetics of adsorption was studied based on experimental data. Four kinetic models were used including the pseudo-first-order equation [29], the pseudo-second-order equation [30], Elovich equation [31] and intra particle diffusion model [32].

The linear form of pseudo-first-order equation of Lagergren is generally expressed as

$$\log(q_e - q_t) = \log q_e - \frac{k_1 t}{2.303} \tag{2}$$

where q_e and q_t are the sorption capacity at equilibrium (μg g^{-1}) and any time t, respectively, and k_1 is the rate constant of pseudo-first-order (min^{-1}). Based on this model the uptake rate and time are directly proportional to the difference in the saturation concentration and the uptake of solute with time.

The liner form of pseudo-second-order equation is expressed as

$$\frac{t}{q_t} = \frac{1}{k_2 q_e^2} + \frac{t}{q_e} \tag{3}$$

The initial sorption rate, h (μg g^{-1} min^{-1}) can be calculated from following equation.

$$h = k_2 q_e^2 \tag{4}$$

where k_2 is the pseudo-second-order rate constant (μg g^{-1} min^{-1}). This model is based on the adsorbate quantity on the adsorbent.

The Elovich equation is expressed as

$$q_t = \frac{\ln(\alpha\beta)}{\beta} + \frac{\ln t}{\beta} \tag{5}$$

where α is the initial sorption rate of reaction (μg g^{-1} min^{-1}) and β is the sorption constant related to surface coverage and activation energy (g μg^{-1}).

The intra-particle diffusion model equation is expressed as

$$q_t = k_{id} t^{0.5} + C \tag{6}$$

where k_{id} is the intra-particle diffusion rate constant (g μg^{-1} $min^{0.5}$). This model is based on transportation of aqueous ions to the surface of adsorbent and then diffusion into the inside of the particles.

6-2. Thermodynamic Parameters

The activation energy of As(V) adsorption onto the MOCZ can be calculated by the relationships

$$\ln k = \ln k_0 - \frac{E_a}{RT} \tag{7}$$

where k is the rate constant second-order of adsorption (g mol^{-1} min^{-1}), k_0 is the independent temperature factor (g mol^{-1} min^{-1}), E_a is the activation energy of adsorption (kJ mol^{-1}), R is the gas constant (8.13 J mol^{-1} K^{-1}), and T is the solution absolute temperature (K). A plot of ln k vs. 1/T gives a straight line, and the corresponding activation energy was determined from the slope of the linear plot.

Thermodynamic parameters such as change in free energy (ΔG^o), enthalpy (ΔH^o) and entropy (ΔS^o) for adsorption reaction were calculated using the following equations:

$$\ln\left(\frac{k}{T}\right) = \left[\ln\left(\frac{K_B}{h_P}\right) - \frac{\Delta H^o}{RT}\right] \tag{8}$$

$$\Delta G^o = RT \ln K_D \tag{9}$$

where k_B is the Boltzmann constant (1.3807×10^{-23} J K^{-1}), h_P is the Planck constant (6.6261×10-34 J s), k is the pseudo-second-order constant (k_2) for As(V) adsorption onto MOCZ, ΔG^o is change in entropy (kJ mol^{-1}) and K_D is distribution coefficient (q_e/C_e). The plot of ln K/T vs 1/T was a straight line and ΔH^o parameter can be calculated from the slope of the linear plot [33-37].

6-3. Sorption Isotherm Models

To describe the interaction between adsorbate and adsorbent, surface properties as well as the degree of affinity of the adsorbent, various isotherm models were used. The linear form of Langmuir's isotherm model [38] is given by the following equation:

$$\frac{C_e}{q_e} = \frac{1}{bQ_{max}} + \frac{C_e}{Q_{max}} \tag{10}$$

where Q_{max} is the amount of As(V) adsorbed at complete monolayer (μg/g) and b is the Langmuir constant related to the binding site (L/μg). The essential characteristics of the Langmuir isotherm commonly known as separation factor or equilibrium parameter (R_L) can be defined as:

$$R_L = \frac{1}{1 + bC_0} \tag{11}$$

where b is the Langmuir constant and C_0 is the highest initial concentration of As(V) ions (μg/L). The value of R_L indicates adsorption nature to be either unfavorable (R_L>1), linear (R_L=1), favorable (0<R_L<1) or irreversible (R_L=0).

The Freundlich isotherm [39] equation can be written in the linear form as given below:

$$\log q_e = \log k_F + \frac{1}{n}\log C_e \tag{12}$$

where k_F [(μg g^{-1}) (L/g)$^{-1/n}$] and n are the Freundlich constants that are related to the adsorption capacity and intensity, respectively.

The liner form of Dubinin-Radushkevich (D-R) isotherm has been expressed by Eq. (13):

$$\ln Q = \ln Q_m - B_{DR}\varepsilon^2 \tag{13}$$

where ε (Polanyi potential)=RT ln (1+1/C_e), Q the amount of arsenic adsorbed at equilibrium per unit weight of MOCZ (μg g^{-1}), Q_m the theoretical saturation capacity, C_e the equilibrium concentration of arsenic in solution (μg L^{-1}), and B_{DR} the D-R model constant (mol^2 kJ^{-2}) [38].

7. Desorption Equilibrium Test

The reversibility of the adsorption of As(V) on MOCZ was studied by desorption experiments. The MOCZ sample obtained after equilibrium with 1 mg L^{-1} As(V) for 24 h was used in an adsorption test. Once equilibrium was reached, the MOCZ loaded with As(V) was separated from the As(V) solution by filtration. Subsequently, the zeolite sample (1 g) was mixed separately with 100 ml of HCl and NaOH solutions (1, 2 and 3 M) for 24 h at room temperature. The mass of the As(V) that remained adsorbed on MOCZ was calculated by a mass balance.

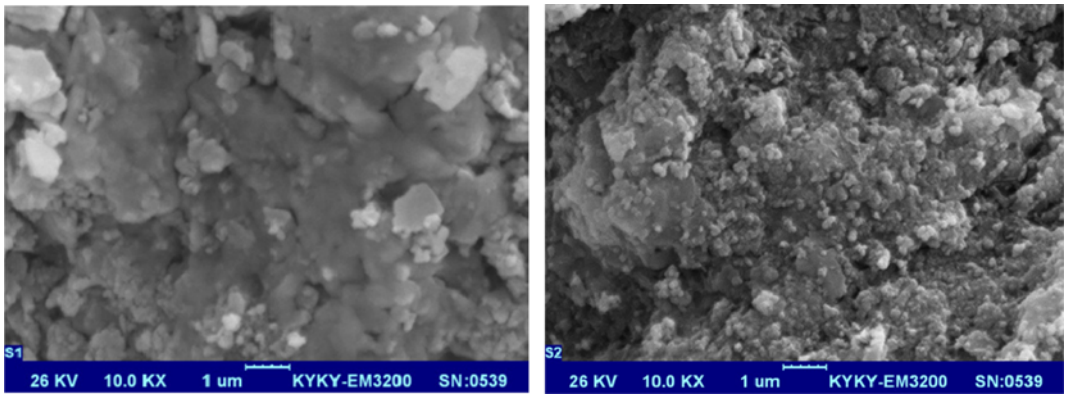

Fig. 1. SEM images of zeolitic tuffs (S1) Raw zeolite, (S2) MnO_2-coated zeolite.

RESULTS AND DISCUSSION

1. Adsorbent Characteristics

Fig. 1 shows that zeolite surface sites were apparently occupied with newborn manganese oxide. A clear difference in the surface morphology of MOCZ may be related to manganese oxide particles that appear to be growing together in surface depressions and coating cracks. SEM image of MOCZ shows many aggregated small particles with much rougher surface that indicates manganese oxide coating.

The x-ray diffractogram pattern obtained for MOCZ sample is shown in Fig. 2. According to XRD analysis, clinoptilolite was the major crystalline phase (~70%). It was found that peaks of clinoptilolite in XRD pattern are in good agreement with data of clinoptilolite. Feldspar sanidine (~19%), quartz (~8%) and ramsdellite (~3%) were also detected in XRD analysis. The oxide coated on zeolite surface is presented as ramsdellite (manganese (IV) oxide) with chemical formula of Mn_1O_2.

The FTIR spectrum of clinoptilolite was taken before and after adsorption to obtain information about the nature of probable interactions between the functional groups on the surface of clinoptilolite and As(V) ions. The results are shown in Fig. 3. The FTIR spectrum does not show significant change in the bulk solid phase, and the only change observed between the spectra is the width of the adsorption bonds. The bonds become wider after adsorption process. The discrete bonds at 3,500 and 1,640 cm^{-1} are due to the water adsorption in the zeolite and significantly hydrated. The spectra bonds at 3,450 and 1,633 cm^{-1} reflect the bending vibration water molecules associated with NA and Ca in the channels of the zeolite. The bonds at 799 and 471 cm^{-1} may be defined as asymmetric stretching vibration mode of O-T-O (T=Si and Al) groups and the bending vibration mode of T-O, respectively. The bond at 1,111 cm^{-1} may be attributed to asymmetric stretching vibration mode of internal T-O bonds in TO_4 tetrahedra [41].

The pH of the point of zero charge, pH_{pzc}, is the point which surface charge density is equal to zero. The MOCZ has a pH_{pzc} equal to 3.6; therefore, its surface has ans acidic character. This value is almost near to the pH_{pzc} reported by Taffarel and Rubio [25]. The

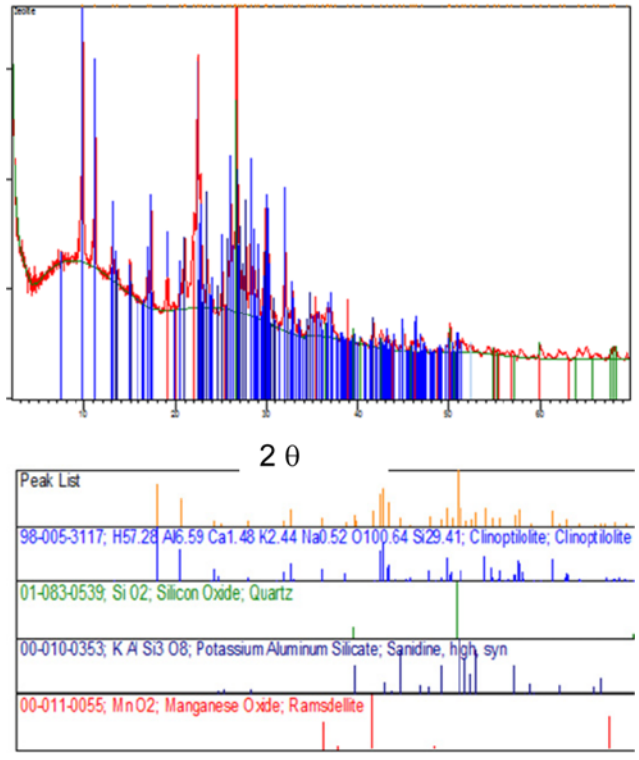

Fig. 2. X-ray diffractogram of the MOCZ sample.

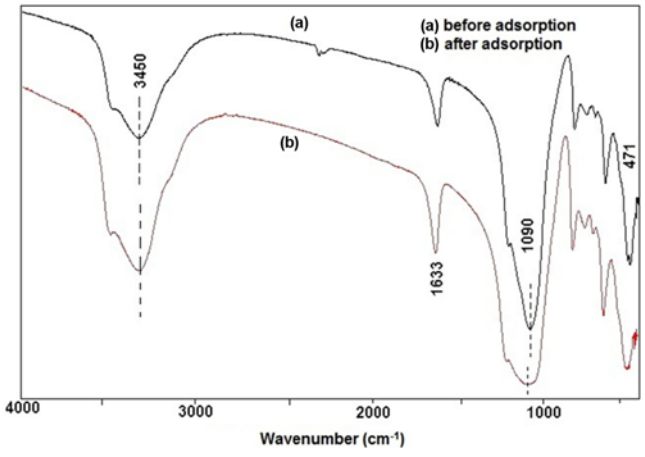

Fig. 3. FTIR spectrum of MOCZ before and after adsorption.

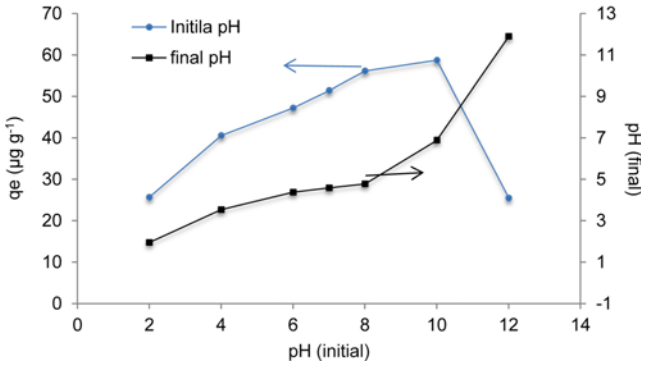

Fig. 4. Effect of pH on the adsorption of As(V) onto MOCZ and pH change after adsorption (C_0=1 mg L^{-1}, t=180 min; C_{MOCZ}= 10 g L^{-1}; T=18 °C).

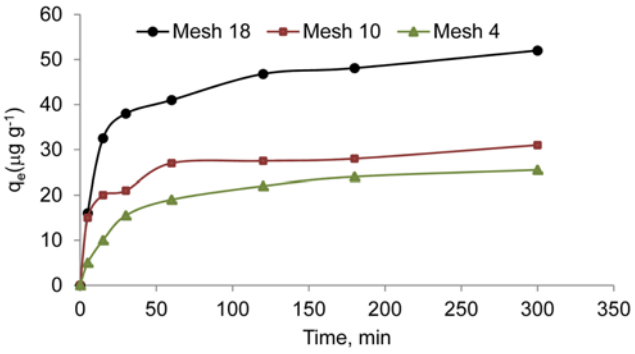

Fig. 5. Amount of As(V) sorbed per unit mass (q_e) of MOCZ at 18 °C with three particle size.

pH_{PZC} of sorbents depends on different factors such as nature of crystallinity, Si/Al ratio, impurity contents, temperature, sorbability of the electrolytes and degree of H^+ and OH^- ions adsorption, and therefore may vary among different adsorbents [42].

2. Effect of Initial pH

Adsorption of As(V) onto MOCZ varied with the initial pH of As(V) solution. Fig. 4 shows the As(V) adsorption by MOCZ over a range of pH 2-12. MOCZ adsorb As(V) effectively over a wide initial pH range of 6-10. At this pH range $H_2AsO_4^-$ and $HAsO_4^{2-}$ are dominant As(V) specie [15]. These two arsenate forms get adsorbed to MnO_2 coated zeolite by Eq. (14).

$$2MCZ-Mn-OH+H_3AsO_4 \rightarrow MCZ_2-(MnO)_2AsOOH+2H_2O \quad (14)$$

where $(MnO)_2AsOOH$ represents the As(V) surface complex. However, there is little information about the As(V) complex that is produced on the surface of zeolite [41].

The pH value at the end of experiments decreased because of ion exchange, surface complex formation and also protonated groups like $AlOH^+$ produced hydrogen ions and lowered the medium pH. The final pH is almost constant for solution with an initial pH ranging between 6 to 8. At strong acidic condition As(V) is present in neutral form and therefore the sorption efficiency is low. Also, at strong alkaline condition (pH 12) the surface of MOCZ becomes negatively charge and electrostatic repulsion between oxyanions of As(V) and zeolite surface decreases the removal. Our results are comparable with the result reported by Chutia et al. [13], Maliykkal et al. [23] and Jeon et al. [44].

3. Effect of Time on Different Particle Size and Sorption Kinetics

The effect of time on arsenic sorption efficiency of different particle size is shown in Fig. 5. As can be seen, at a fixed MOCZ dose (1 g/100 ml) and arsenate concentration (1 mg L^{-1}) the time required to reach an equilibrium state is short for smaller size particles. So, the amount of required adsorbate can reduce significantly at the same dose. The adsorption of As(V) ions reaches equilibrium in 80, 120 and 180 min for particle size 18, 10 and 4 mesh, respectively. However, the optimum agitation time was fixed at 180 min through this study. Since, adsorption is a surface phenomenon, higher adsorption of As(V) by 18 mesh (52%) compared to 4 mesh (24%) at equilibrium is related to larger surface area per unit weight

Table 1. Kinetic parameters for the adsorption of As(V) by MOCZ

Model/factor		$q_{e,exp}$ (µg g^{-1})	Pseudo-first-order kinetic model			Pseudo-second-order kinetic model			
			$K_1\times10^{-2}$	q_1 (µg g^{-1})	R^2	$K_2\times10^{-3}$	q_2 (µg g^{-1})	h	R^2
Particle size (mesh)	18	48.2	3.02	32.89	0.974	1.85	50.77	4.8	0.997
	10	28.1	2.69	12.08	0.888	4.94	29.0	4.19	0.997
	4	24.1	2.73	23.78	0.949	1.56	26.9	1.33	0.985
T (K)	291	48.2	3.14	32.89	0.974	2.09	49.4	5.12	0.997
	301	54.1	2.93	31.34	0.890	2.16	56.2	6.81	0.998
	311	60.1	2.96	35.88	0.952	2.03	62.1	7.84	0.997

Model/factor		$q_{e,exp}$ (µg g^{-1})	Intraparticle diffusion model			Elovich equation		
			K_{id}	C	R^2	α	β	R^2
Particle size (mesh)	18	48.2	1.98	21.87	0.811	8.16	7.11	0.943
	10	28.1	1.12	14.87	0.75	3.81	9.22	0.920
	4	24.1	1.62	4.04	0.933	5.42	3.78	0.992
T (K)	291	48.2	1.81	22.78	0.794	7.57	8.73	0.93
	301	54.1	1.87	28.30	0.778	7.98	13.31	0.937
	311	60.1	2.22	31.72	0.765	8.76	16.74	0.974

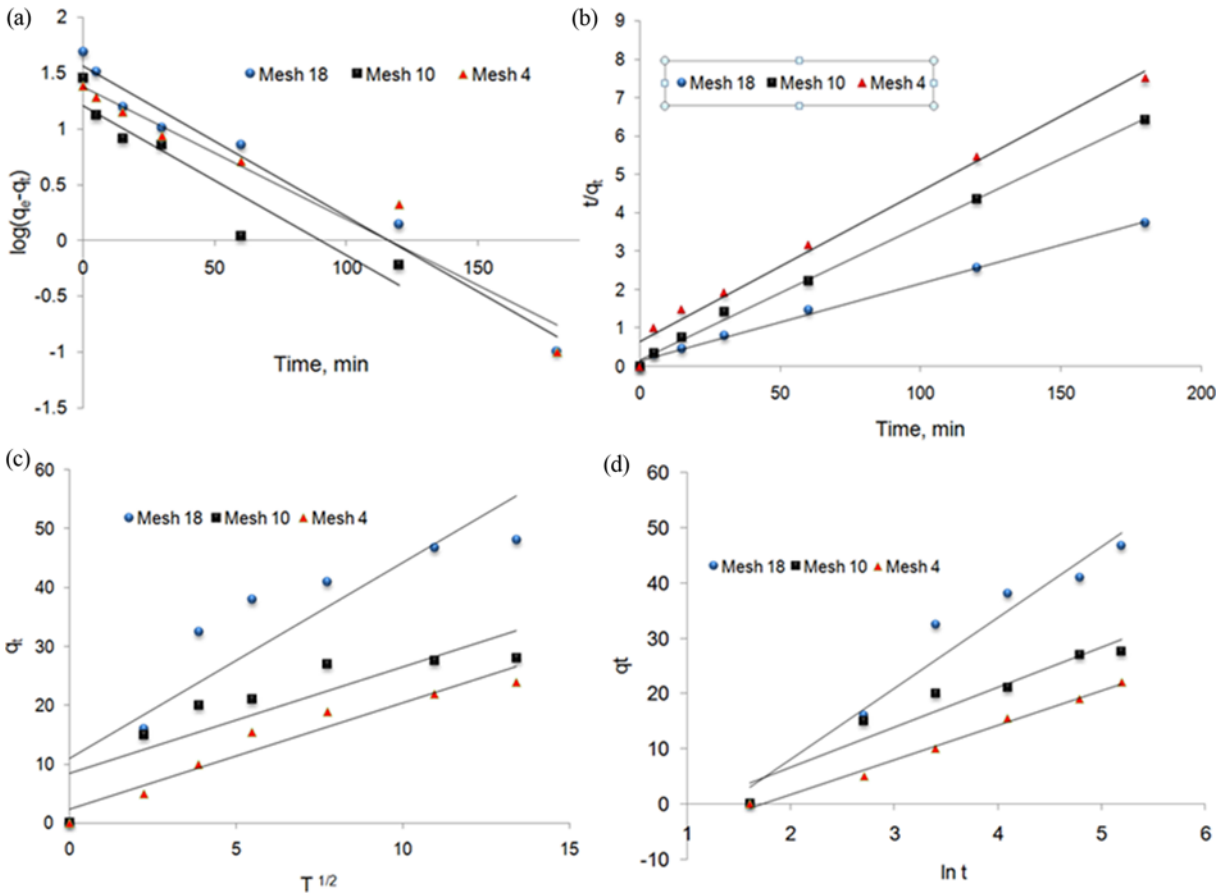

Fig. 6. Kinetic plots for As(V) adsorption (a) pseudo-first-order (b) pseudo-second-order (c) intraparticle model (d) elovich model.

and more accessibility to pore of the adsorbent. Generally, kinetics of adsorption consists of two phases: an initial rapid phase and a relative slow phase. The first one was due to the abundant availability of sorption sites in MOCZ, and the other one was due to quick saturation of the adsorption sites [45,46].

To determine the efficacy of adsorption and identify the adsorption mechanism, chemical reaction rate and potential rate controlling steps, kinetic models have been investigated. The experimental data were fitted to four kinetics models and results are shown in Table 1 and Fig. 6. The models were evaluated based on correlation coefficient, R^2. Based on R^2 value, arsenate ions adsorption on the MOCZ did not follow a pseudo-first-order reaction. Moreover, the $q_{e(theor)}$ values had a large difference with $q_{e(exp)}$ value and are less than $q_{e(exp)}$. According to Febrianto et al. [47], the $q_{e(theor)}<q_{e(exp)}$ caused by the presence of boundary layer or external resistance was controlling the beginning of the sorption process.

The pseudo-second-order kinetic model has higher correlation coefficient ($R^2>0.985$) than the others and $q_{e(thero)}$ agrees very well with the $q_{e(exp)}$. So, the adsorption behavior can be interpreted very well by this kinetic model over the whole range of contact time. This suggested that the rate limiting step in adsorption of As(V) ions is chemisorption such as complexation, change of electron between sorbate and sorbent and coordination [45,48,49].

Overall, from Table 1 the value of correlation coefficient decreases from pseudo-second-order, Elovich equation, pseudo-first-order and intraparticle diffusion. However, it was observed that intraparticle diffusion plays less significant role in the adsorption process. This finding is similar to Moussavi and Khosravi [50] who used three kinetic equations (pseudo 1st, 2nd and intraparticle diffusion) to describe cyanide sorption onto pistachio hull waste.

4. Thermodynamic Study

The kinetic parameters of various kinetic models and correlation coefficient (R^2) under different temperature are summarized in Table 1. The pseudo-second-order has the highest correlation

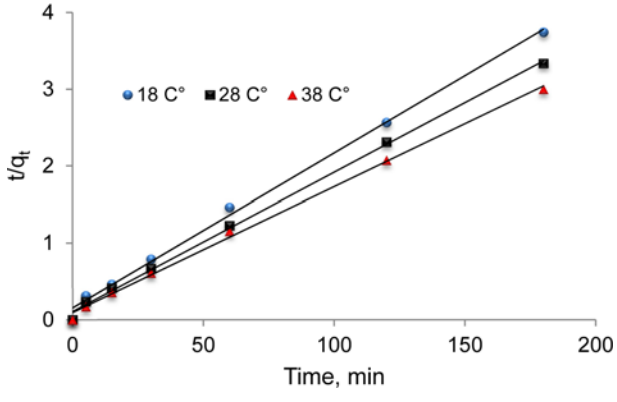

Fig. 7. Pseudo-second-order sorption kinetics of As(V) ions on MOCZ with different temperatures.

Table 2. Thermodynamic parameters of the adsorption process

T (K)	ΔG^o (kJ mol^{-1})	ΔH^o (kJ mol^{-1})	ΔS^o (kJ mol^{-1} K^{-1})	E_a (kJ mol^{-1})
291	−83.9			
301	−86.7	1.18	−0.29	3.68
311	−89.8			

coefficient (R^2>0.99) in this study. The linear plots of t/q_t vs t for pseudo-second-order model for different temperature are shown in Fig. 7. The theoretical $q_{e(theor)}$ and the initial sorption rate, h, increased with increasing of temperature. This result clearly indicates that high temperature favors As(V) adsorption onto MOCZ.

To calculate the activation energy (E_a), the linearized Arrhenius equation Eq. (7) was applied, and results of thermodynamic parameters such as ΔH^o, ΔS^o and ΔG^o are summarized in Table 2. The value of E_a was found to be 3.68 kj mol^{-1}, indicating that the adsorption process may be a physical adsorption. The positive value also indicates an endothermic reaction. The positive value of differential heat of adsorption (ΔH^o) suggests that the adsorption of As(V) onto the MOCZ is an endothermic process, i.e., the q_e increases with increasing T. The negative standard entropy change (ΔS^o) value implies a decrease in the degree of freedom of the adsorbed ions. ΔG^o values were negative at all of the temperatures (291-311 K), indicating that adsorption of arsenate onto MOCZ was spontaneous and thermodynamically favorable.

5. Equilibrium Isotherms

An isotherm describes the relationship of the concentration of an adsorbate between two separate phases at equilibrium at a constant temperature. So, here the relationship between the amount of As(V) ions adsorbed onto MOCZ at given experimental condition in liquid phase was described by isotherm. Moreover, the equation parameters of isotherm models often provide an insight into the adsorption mechanism, surface properties and affinity of the adsorbent [44,48]. In this study, three of the most used isotherm models (Langmuir, Freundlich and (D-R)) were used to describe experimental data. Fig. 8 shows the As(V) adsorption isotherms onto MOCZ, and the values of the constants and correlation coefficients (R^2) are summarized in Table 3.

The Langmuir isotherm model has traditionally been used to describe the interaction between the adsorbate concentration to the active sites on the surface of adsorbent at equilibrium [51]. The model assumes that all active sites have equal affinity for the sorbate, and once the molecule or ion occupies the adsorption site, no further adsorption can take place [49,50]. Moreover, there is no dependency between the adsorption of a molecule to a given site on the neighboring sites [48]. In Fig. 8(a), q_e values increased with increasing of nitrate concentration. Langmuir isotherm plots for As(V) adsorption on MOCZ at 18, 28 and 38 °C are shown in Fig. 8(b). The values of Langmuir constant (b) were found to be 0.88, 0.96 and 1.17 L μg^{-1} at 18, 28 and 38 °C (Table 3) indicating good affinity between the sorbent and sorbate at all temperatures. The b values increased with increasing temperature, which implies that the sorption process is endothermic. According to Ngah and Yosop [46], this phenomenon leads to physisorption of the adsorption process, which with increasing temperature the bonding becomes

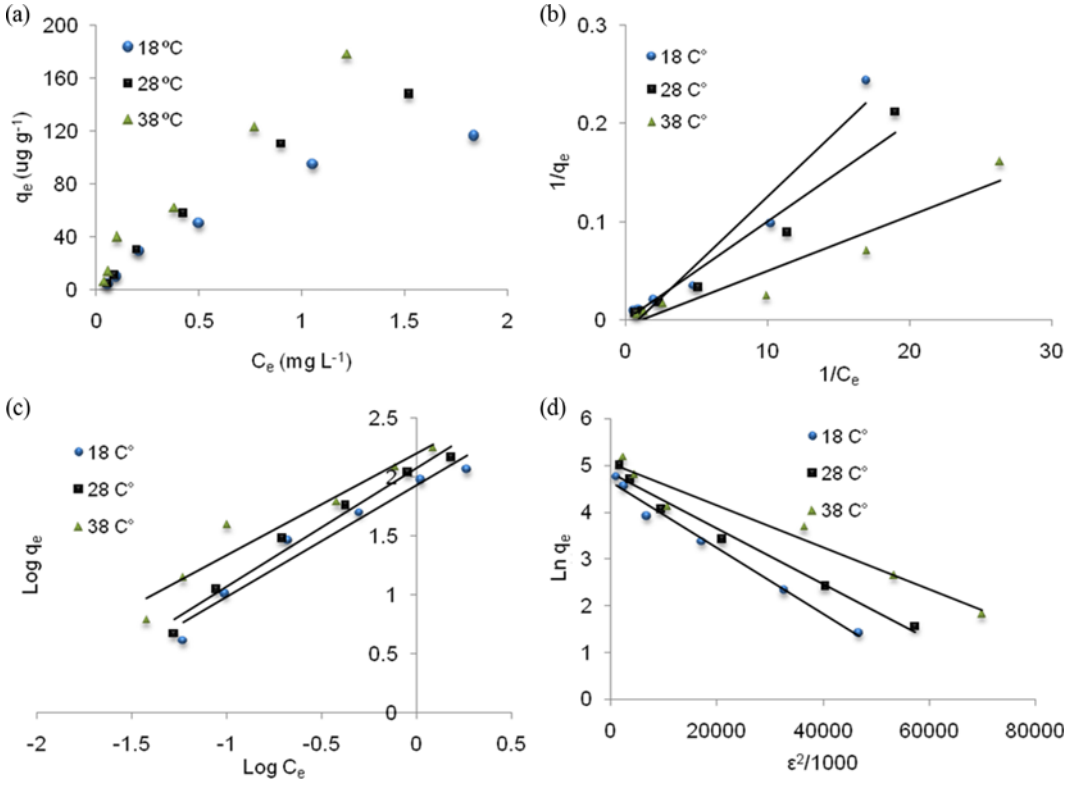

Fig. 8. (a) The adsorption of arsenic (V) on the MOCZ; (b) Linear plots of isotherm models of Langmuir; (c) Freundlich; (d) Dubinin-Radushkevich for adsorption of As(V) onto MOCZ. pH 7; contact time 180 min; MOCZ dose 10 g L^{-1}.

Table 3. Adsorption isotherm parameters for adsorption of As(V) on MOCZ at different temperatures

Isotherm equation		T		
		291 K	301 K	311 K
Langmuir	Q_{max} (μg g^{-1})	82.59	96.35	150.9
	b (L μg^{-1})	0.88	0.96	1.17
	R_L	0.28	0.23	0.22
	R^2	0.95	0.954	0.919
Freundlich	K_F [(μg g^{-1}) $(L/g)^{-1/n}$]	85.5	126.02	160.2
	n	1.06	1	1.16
	R^2	0.955	0.933	0.975
D-R	Q_m (μg g^{-1})	103.69	126.48	152.8
	E (kJ mol^{-1})	2.66	2.9	3.48
	R^2	0.986	0.959	0.981

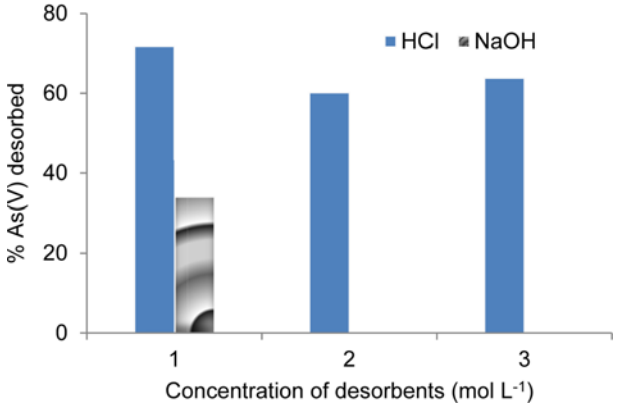

Fig. 9. The desorption of As(V) from saturated MOCZ (C_0=1 mg L^{-1}, t=24 h).

weaker. The values of maximum monolayer adsorption capacity, Q_{max}, were 82.69, 96.35 and 150.9 μg g^{-1} at mentioned temperatures. These adsorbed values were more higher compared to the value reported by Camacho, Parra and Deng [22] 2.5 μg g^{-1}; Fierro et al. [53] 28 μg g^{-1}; for initial arsenic concentration 0.3 mg L and Pokhrel and Viraraghavan [54], 42.6 μg g^{-1}. The essential feature of the Langmuir isotherm, commonly known as the separation factor or equilibrium parameter (R_L), was in the range of 0.22-0.28. This indicated that adsorption was favorable at all temperatures. Moreover, at higher concentration the R_L value was lower, indicating that the adsorption was more favorable [50].

The Freundlich isotherm model is derived by assuming a non-ideal adsorption on heterogeneous surface with a multilayer adsorption [53]. As the adsorption process becomes completed the energies of adsorption decrease exponentially. Fig. 8(c) shows the Freunlich isotherm plots calculated at various temperatures for the As(V) adsorption onto MOCZ. Based on Table 3, high correlation coefficients (R^2) were found with this model, showing that the equilibrium data fit well with Freundlich model. Also, this implies that the MOCZ has specification of heterogeneous adsorption site. The n values were just above than 1 which indicated that the arsenate was favorably adsorbed by MOCZ [55]. The K_F value increased from 85.5 at 18 °C to 160.2 at 38 °C, respectively, which implied that adsorption capacity increased with increases in temperature, and at higher temperatures the heterogeneous adsorption sites played a more important role.

Based on table, the highest correlation coefficients (R^2) belonged tothe D-R isotherm. This isotherm determines a high degree of regularity, adsorption type and the mechanism [50,54]. The D-R constants were calculated and represented in Table 3 and Fig. 8(d) shows the D-R isotherm plot. The mean free energy[E(kj mol^{-1})], per mole or ion of adsorbate (change in free energy when one ion transport from its location to the sorption site) can be determined by this equation [38].

$$E = \left[\frac{1}{\sqrt{2B_{DR}}}\right] \quad (14)$$

where B_{DR} is an isotherm constant related to adsorption energy. The value of mean free energy (E) can be used to estimate chemical and physical sorption. If E value is in the range of 1 to 8 kj mol^{-1} the sorption is physical, and between 8 to 16 kj mol^{-1} is chemical [50,53-56]. The values of E found in this study (2.66-3.48 kj mol^{-1}) were lower than 8, indicating that adsorption is physical, which is due to weak van der Waals force.

6. Reversibility of As(VI) Adsorption on MOCZ

The reversibility of any exhausted adsorbent is a critical aspect in the sorption process for improving the process economics [59]. In this study various concentrations of HCl and NaOH were used for arsenic desorption from exhausted MOCZ. It was revealed that arsenic could not be desorbed in the presence of NaOH. By contrast, HCl could elute 60-71% of sorbed As(V) from MOCZ (Fig. 9). However, low acidic solutions can be used for the regeneration of MOCZ.

CONCLUSIONS

The present study shows that permanganate-modified zeolite is an effective sorbent for removal of arsenic from aqueous solution. The availability of natural clinoptilolite in nature, low cost, high initial sorption rate and good sorption efficiency at wide pH range make this material suitable for potential practice applications. The optimum removal pH ranked from 6-10 and because pH value of groundwater is generally between 6.5 and 8; therefore, MOCZ can be used effectively. Adsorption capacity increased with increasing temperature. Various kinetic models were used to describe the adsorption process. The kinetics data were best described by pseudo-second-order equation. The thermodynamic parameters indicated that the adsorption process is endothermic and spontaneous. The equilibrium of sorption follows Langmuir, Freundlich and D-R isotherms well. The result suggested that the sorption could be due to physical interaction such as van der Waals interaction and surface adsorption. The chemical interaction may also play a role in the process. From a dimensionless equilibrium parameter (R_L) it is concluded that desorption is favorable and that MOCZ has great ability to absorb arsenic.

REFERENCES

1. M. Jiménez-Cedillo, M. Olguín and C. Fall, *J. Hazard. Mater.*, **163**(2),

939 (2009).
2. R. Menhage-Bena, H. Kazemian, M. Ghazi-Khansari, M. Hosseini and S. Shahtaheri, *Iran. J. Public Health*, **33**(1), 36 (2004).
3. K. B. Vu, M. D. Kaminski and L. Nunez, *Review of arsenic removal technologies for contaminated groundwaters*, in *Other Information: PBD: 2 May* 2003. 2003. p. Medium: ED; Size: 43 pages.
4. T. Stanić, A. Daković, A. Živanović, M. Tomašević-Čanović, V. Dondur and S. Milićević, *Environ. Chem. Lett.*, **7**(2), 161 (2009).
5. M. S. Rahaman, A. Basu and M. R. Islam, *Bioresour. Technol.*, **99**(8), 2815 (2008).
6. M. Šiljeg, L. Foglar and I. Gudelj, *Chem. Ecol.*, **28**(1), 75 (2011).
7. T. K. Dora, Y. K. Mohanty, G. K. Roy and B. Sarangi, *J. Environ. Chem. Eng.*, **1**(3), 150 (2013).
8. M. F. Naujokas, B. Anderson, H. Ahsan, H. V. Aposhian, J. H. Graziano, C. Thompson and W. A. Suk, *Environ. Health Perspect.*, **121**(3), 295 (2013).
9. P. Chutia, S. Kato, T. Kojima and S. Satokawa, *J. Hazard. Mater.*, **162**(1), 440 (2009).
10. M. Mosaferi, et al., Occurrence of arsenic in Kurdistan Province of I.R. Iran, Proceeding of Conference on Fate of Arsenic in the Environment, 1 (2003).
11. A. Dominguez-Ramos, K. Chavan, V. García, G. Jimeno, J. Albo, K. V. Marathe, G. D. Yadav and A. Irabien, *Ind. Eng. Chem. Res.*, **53**(49), 18920 (2014).
12. H. Elcik, M. Cakmakci, E. Sahinkaya and B. Ozkaya, *Ind. Eng. Chem. Res.*, **52**(29), 9958 (2013).
13. X. Dou, D. Mohan and C. U. Pittman Jr., *Water Res.*, **47**(9), 2938 (2013).
14. E. Lacasa, C. Sáez, P. Cañizares, F. J. Fernández and M. A. Rodrigo, *Sep. Sci. Technol.*, **48**(3), 508 (2012).
15. P. Chutia, S. Kato, T. Kojima and S. Satokawa, *J. Hazard. Mater.*, **162**(1), 204 (2009).
16. Z. Li, J.-S. Jean, W.-T. Jiang, P.-H. Chang, C.-J. Chen and L. Liao, *J. Hazard. Mater.*, **187**(1-3), 318 (2011).
17. M. Baskan and A. Pala, *Water, Air, Soil Pollut.*, **225**(1), 1 (2013).
18. M. Qiu, Q. Jian, D. Yu and K. Feng, *Desalination and Water Treatment*, **24**(1-3), 61 (2010).
19. A. Olad, S. Ahmadi and A. Rashidzadeh, *Desalination and Water Treatment*, **51**(37-39), 7172 (2013).
20. A. A. Zorpas, *Desalination and Water Treatment*, **8**(1-3), 256 (2009).
21. A. Nezamzadeh-Ejhieh and M. Shahanshahi, *J. Ind. Eng. Chem.*, **19**(6), 2026 (2013).
22. L. M. Camacho, R. R. Parra and S. Deng, *J. Hazard. Mater.*, **189**(1-2), 286 (2011).
23. S. M. Maliyekkal, L. Philip and T. Pradeep, *Chem. Eng. J.*, **153**(1-3), 101 (2009).
24. S.-X. Teng, S.-G. Wang, W.-X. Gong, X.-W. Liu and B.-Y. Gao, *J. Hazard. Mater.*, **168**(2-3), 1004 (2009).
25. S. R. Taffarel and J. Rubio, *Min. Eng.*, **23**(14), 1131 (2010).
26. S. Bajpai and M. Chaudhuri, *J. Environ. Eng.*, **125**(8), 782 (1999).
27. P. C. C. Faria, J. J. M. Órfão and M. F. R. Pereira, *Water Res.*, **38**(8), 2043 (2004).
28. J. Rivera-Utrilla, I. Bautista-Toledo, M. A. Ferro-García and C. Moreno-Castilla, *J. Chem. Technol. Biotechnol.*, **76**(12), 1209 (2001).
29. Y. S. Ho and G. McKay, *Process Safety and Environmental Protection*, **76**(4), 332 (1998).
30. Y. S. Ho and G. McKay, *Chem. Eng. J.*, **70**(2), 115 (1998).
31. M. J. D. Low, *Chem. Rev.*, **60**(3), 267 (1960).
32. N. Chiron, R. Guilet and E. Deydier, *Water Res.*, **37**(13), 3079 (2003).
33. W. Zou, R. Han, Z. Chen, Z. Jinghua and J. Shi, *Colloids Surf., A: Physicochemical and Engineering Aspects*, **279**(1-3), 238 (2006).
34. A. Sarı, D. Çıtak and M. Tuzen, *Chem. Eng. J.*, **162**(2), 521 (2010).
35. K. Banerjee, G. L. Amy, M. Prevost, S. Nour, M. Jekel, P. M. Gallagher and C. D. Blumenschein, *Water Res.*, **42**(13), 3371 (2008).
36. M. Al-Ghouti, M. A. M. Khraisheh, M. N. M. Ahmad and S. Allen, *J. Colloid Interface Sci.*, **287**(1), 6 (2005).
37. Y. Bulut and H. Aydın, *Desalination*, **194**(1-3), 259 (2006).
38. I. Langmuir, *J. Am. Chem. Soc.*, **38**(11), 2221 (1916).
39. F. Gimbert, N. Morin-Crini, F. Renault, P.-M. Badot and G. Crini, *J. Hazard. Mater.*, **157**(1), 34 (2008).
40. K. Y. Foo and B. H. Hameed, *Chem. Eng. J.*, **156**(1), 2 (2010).
41. H. Tanaka, N. Yamasaki, M. Muratani and R. Hino, *Mater. Res. Bulletin*, **38**(4), 713 (2003).
42. I. D. Smičiklas, S. K. Milonjić, P. Pfendt and S. Raičević, *Sep. Purif. Technol.*, **18**(3), 185 (2000).
43. B. A. Manning, S. E. Fendorf, B. Bostick and D. L. Suarez, *Environ. Sci. Technol.*, **36**(5), 976 (2002).
44. C.-S. Jeon, K. Baek, J.-K. Park, Y.-K. Oh and S.-D. Lee, *J. Hazard. Mater.*, **163**(2-3), 804 (2009).
45. M. Ahmad, S. Lee, S.-E. Oh, D. Mohan, D. Moon, Y. Lee and Y. Ok, *Environ. Sci. Pollut. Res.*, **20**(12), 8364 (2013).
46. W. S. W. Ngah, S. Fatinathan and N. A. Yosop, *Desalination*, **272**(1-3), 293 (2011).
47. J. Febrianto, A. N. Kosasih, J. Sunarso, Y.-H. Ju, N. Indraswati and S. Ismadji, *J. Hazard. Mater.*, **162**(2-3), 616 (2009).
48. I. A. Oke, N. O. Olarinoye and S. R. A. Adewusi, *Adsorption*, **14**(1), 73 (2008).
49. X.-j. Wang, S.-q. Xia, L. Chen, J.-f. Zhao, J.-m. Chovelon and J.-r. Nicole, *J. Environ. Sci.*, **18**(5), 840 (2006).
50. G. Moussavi and R. Khosravi, *J. Hazard. Mater.*, **183**(1-3), 724 (2010).
51. T. Khan, S. Chaudhry and I. Ali, *Environ. Sci. Pollut. Res.*, **20**(8), 5425 (2013).
52. K. Vijayaraghavan, T. V. N. Padmesh, K. Palanivelu and M. Velan, *J. Hazard. Mater.*, **133**(1-3), 304 (2006).
53. V. Fierro, G. Muñiz, G. Gonzalez-Sánchez, M. L. Ballinas and A. Celzard, *J. Hazard. Mater.*, **168**(1), 430 (2009).
54. D. Pokhrel and T. Viraraghavan, *Sep. Sci. Technol.*, **43**(13), 3545 (2008).
55. S. Saha and P. Sarkar, *J. Hazard. Mater.*, **227-228**, 68-78.
56. S. K. Maji, A. Pal, T. Pal and A. Adak, *J. Surf. Sci. Technol.*, **23**(3-4), 161 (2007).
57. S. Kunzru and M. Chaudhuri, *J. Environ. Eng.*, **131**(9), 1350 (2005).
58. P. Bhunia, A. Pal and M. Bandyopadhyay, *J. Hazard. Mater.*, **141**(3), 826 (2007).
59. R. Leyva-Ramos, A. Jacobo-Azuara, P. E. Diaz-Flores, R. M. Guerrero-Coronado, J. Mendoza-Barron and M. S. Berber-Mendoza, *Colloids Surf., A: Physicochemical and Engineering Aspects*, **330**(1), 35 (2008).